[논 문] 한국재료학회지
Kor. J. Mater. Res.
Vol. 24, No. 10 (2014)
http://dx.doi.org/10.3740/MRSK.2014.24.10.509

Capillary Assembly of Silicon Nanowires Using the Removable Topographical Patterns

Juree Hong, Seulah Lee, Sanggeun Lee, Jungmok Seo and Taeyoon Lee†

Nanobio Device Laboratory, School of Electrical and Electronic Engineering, Yonsei University, 50 Yonsei-ro, Seodaemun-gu, Seoul 120-749, Korea

(Received July 8, 2014 : Received in revised form August 26, 2014 : Accepted August 26, 2014)

Abstract We demonstrate a simple and effective method to accurately position silicon nanowires (Si NWs) at desirable locations using drop-casting of Si NW inks; this process is suitable for applications in nanoelectronics or nanophotonics. Si NWs were assembled into a lithographically patterned sacrificial photoresist (PR) template by means of capillary interactions at the solution interface. In this process, we varied the type of solvent of the SiNW-containing solution to investigate different assembly behaviors of Si NWs in different solvents. It was found that the assembly of Si NWs was strongly dependent on the surface energy of the solvents, which leads to different evaporation modes of the Si NW solution. After Si NW assembly, the PR template was cleanly removed by thermal decomposition or chemical dissolution and the Si NWs were transferred onto the underlying substrate, preserving its position without any damage. This method enables the precise control necessary to produce highly integrated NW assemblies on all length scales since assembly template is easily fabricated with top-down lithography and removed in a simple process after bottom-up drop-casting of NWs.

Key words silicon nanowire, silicon nanowire assembly, topographical patterns, capillary force.

1. Introduction

One-dimensional silicon nanowires(SiNWs) have been extensively researched over the past few decades, owing to its high carrier mobilities with excellent mechanical, which arises from their miniaturized dimensions.[1-5] To take advantage of their unique physical properties, however, uniform assembly of these nanostructures in large-scale with desired patterns is highly necessitated. Several reports have demonstrated methods to assemble NWs into desired structures, including the electric/magnetic field assisted assembly method,[6,7] fluidic flow as-sembly method,[8-9] stick-slip motion method,[10,11] Langmuir-Blodgett method,[12-15] contact printing method,[16,17] and selection adhesion method.[18-20] Although such aforementioned methods have shown considerable progresses in assembling SiNWs into desired positions, they generally require unconventional facilities and sophisticated treatments which can be major problematic in cost-effectiveness and simplicity of the fabrication process.

Here, we demonstrate a facile and effective method to selectively locate SiNWs in pre-defined patterns, which comprises of the following simple steps: drop-cast of SiNW solution onto lithographically patterned photoresist (PR) templates and subsequent removal of the PR templates. It was observed that the assembly behavior of the SiNWs on the patterned substrate was strongly dependent on the surface energy of the solvents which leads to different evaporation modes of the SiNW solution. When a solvent with high surface energy was used, the evaporation mode was de-pinned mode; the contact angle between the SiNW-containing droplet and the patterned substrate remains constant, while the contact area gradually decreased during the evaporation. When the receding contact line of the droplet encountered the underlying patterns on the substrate, the SiNW solution was trapped at the pre-defined patterns due to the local capillary forces. Consequently, the trapped SiNW solutions remaining the pre-defined regions were evaporated and left as an assembled network of SiNWs. On the contrary, the evaporation mode was changed to pinned mode when a solvent with low surface energy was used. In the pinned

†Corresponding author
E-Mail : taeyoon.lee@yonsei.ac.kr (T. Lee, Yonsei Univ.)

mode, the contact area between the SiNW solution and the patterned substrate was maintained constant while the contact angle decreased during the evaporation. Unlike the de-pinned mode where the contact line continuously receded towards the center of the droplet, the contact line was fixed and the SiNWs were randomly deposited on the substrates without any selective assembly at the topographical patterns. After the selective assembly of the SiNWs at the pre-defined regions of the substrate, the PR template could be removed through a rapid thermal annealing process, and it was observed that both the position and orientation of the SiNWs were preserved. The electrical measurements confirmed that the typical two-terminal resistance of the SiNW networks was approximately 500 KΩ, which indicated a good connectivity of the SiNW networks.

2. Experimental Procedure

20-μm-long SiNWs with diameter ranging from 100 to 200 nm were synthesized from a (100) oriented p-type Si substrate (1-10 Ω·cm) using the aqueous electroless etching (AEE) method described in detail elsewhere.[21] In detail, 1×1 cm^2 samples were prepared and cleaned by successive ultrasonication in acetone, IPA, and DI water for 7 minutes each, which were then immersed in a solution mixture of 4.9 M HF and 0.03 M $AgNO_3$ at 60 °C for 60 minutes. The residual silver nanoparticles and byproducts from the etching process were removed by dipping in HNO_3 solution (68 wt%) for 1 minute, followed by a thorough rinsing with DI water and sample drying at ambient conditions. The vertically grown SiNWs via AEE method was observed with a field emission scanning electron microscope(FE-SEM) image(Fig. 1(b)). To obtain well-dispersed SiNW colloidal suspensions, the vertically grown SiNWs were immersed in the target solvents(DI water and IPA) and removed after ultrasonication for 30 seconds. The SiNW suspension was dropped on the SiO_2/Si substrate and evaporated to observe the diameter of SiNWs, which is represented in FE-SEM image in Fig. 1(c).

Fig. 1 illustrates the schematic procedure to obtain well-defined patterns of SiNW networks. SU-8-2002 was patterned on Si substrates with a 200-nm-thick thermally grown SiO_2 layer using a photo mask aligner(MDA-400M, Midas System Co., Ltd.) equipped with UV exposure light source with 350 W. A ~300 μL SiNW colloidal suspension with two sets of colloidal solvents were directly drop-casted on the patterned substrate and dried under air ambient at room temperature. After the entire assembly process was completed, the SU-8-2002 templates were thermally decomposed using a furnace at temperature of 450 °C under oxygen ambient. For electrical measurements, 50-nm-thick Au/10-nm-thick Ti layers were thermally evaporated over a square shadow mask with dimensions of 500×500 μm^2 on the top of the SiNW assemblies.

The entire evaporation process of SiNW colloidal droplet was observed in-situ using an optical microscope with a mounted digital camera(ATCAM 300MI). The electrical transport property of the patterned SiNW assemble network was measured with a Keithley 236 source-measurement unit in a probe station.

3. Results and Discussion

Fig. 2 demonstrates the typical optical micrographs of the formed SiNW assemblies prior to the PR pattern removal. As a preliminary experiment, various solvents were tested to prepare a stable SiNW colloidal suspension, which was critical in the assembly of SiNW networks on the pre-defined patterns of SiO_2/Si substrate. Since the synthesized SiNWs exhibited hydrophilic properties owing

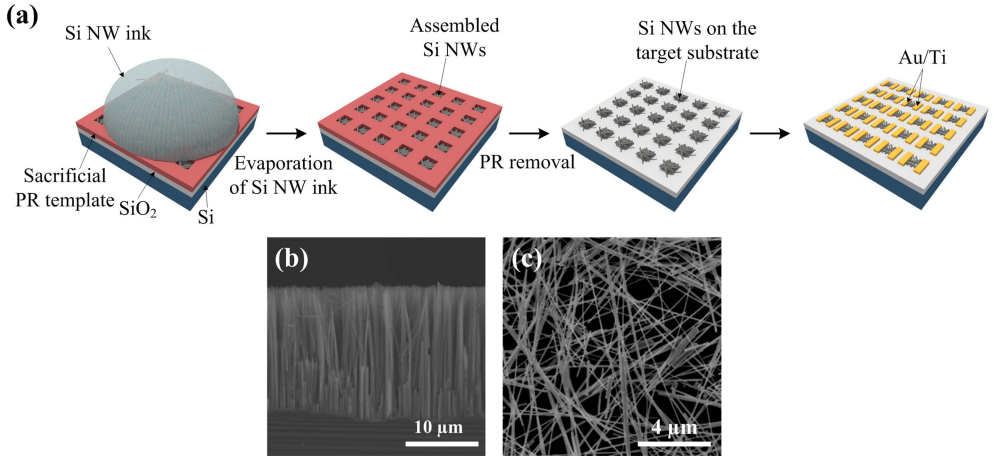

Fig. 1. (a) Fabrication process used to assemble SiNWs on target areas on topographical patterns on SiO_2/Si substrate. FE-SEM micrographs of (b) vertically grown SiNWs via an AEE method, and (c) SiNWs on SiO_2 substrate after evaporation of SiNW inks.

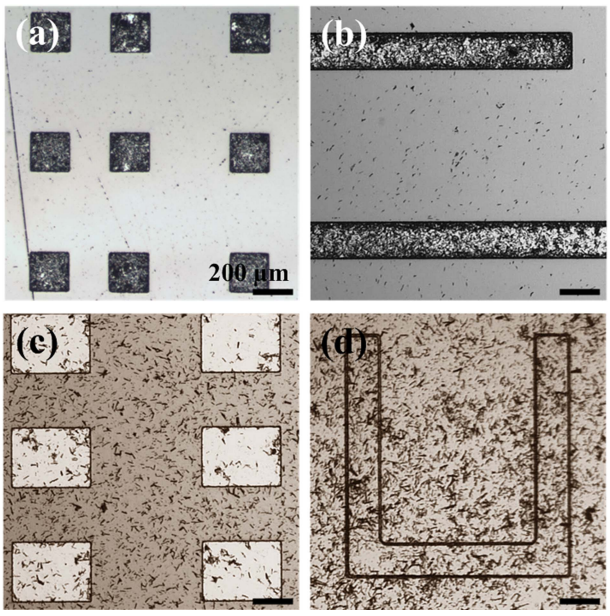

Fig. 2. Optical microscope images of SiNW networks on topographically patterned substrates assembled by using two different solutions: (a) and (b) DI water; (c) and (d) IPA. All scale bars indicate 200 μm.

to the native oxide layer formed on their surfaces, the use of hydrophobic solvents such as toluene and chloroform resulted in an unstable colloidal suspension with high agglomerations of the SiNWs. Thus, we only focused on the assembly of SiNWs using hydrophilic solvents(DI water and IPA). Figs. 2(a) and (b) represent the self-assembled SiNW networks on the square- and line-patterned SiO_2 substrates, respectively, which were obtained from the evaporation of DI water-based SiNW solution. On the other hand, the SiNWs were randomly deposited throughout the patterned surfaces when SiNW solution based on IPA was used, as shown in Figs. 2(c) and (d).

In order to better understand the assembly mechanisms of the SiNWs on the patterned substrates during the evaporation of different SiNW solutions, the evaporation process were observed using an *in-situ* optical microscope. Fig. 3 exhibits the sequential optical images of the evaporation process of DI water-based SiNW ink with respect to evaporation time. Owing to the high surface energy of DI water (72.8 mN/m), a de-pinned evaporation mode was observed when the SiNW solution was drop-casted on the hydrophobic surface of patterned SU-8-2002 on SiO_2/Si substrates. Notably, as the contact area between the SiNW solution and the patterned substrate gradually decreased through the evaporation, the unmasked areas were filled with the SiNW ink, which were separated from the original droplet(Fig. 3(c)). Consequently, the unmasked areas of the SiO_2 substrate were left with assembled network of SiNWs after the full evaporation of the SiNW solution, as already shown in Figs. 2(a) and (b). When the solution was changed to IPA, which had lower surface energy of 21.7 mN/m, the observed evaporation mode was pinned mode when it was drop-casted on the patterned substrate. The contact area between the SiNW solution and the patterned substrate remained, maintaining its perimeter until the evaporation was completed(image not shown). Thus, the SiNW solution could not be selectively filled into the unmasked areas of the SiO_2 substrate, and instead the SiNWs were randomly distributed on the patterned surface.

Fig. 4 schematically illustrates the detailed assembly process of SiNWs on the SU-8-2002 patterned SiO_2/Si substrates using different SiNW solutions. As evidenced from the observations of Fig. 3, the self-assembly mechanism of the SiNWs in solutions were highly associated with the evaporation mode. The de-pinned mode(DI water-based SiNW solution) was occurred because of the high surface tension and slow evaporation rate of the solvent. The contact area between the SiNW ink and the patterned SiO_2/Si substrate continuously decreased during the evaporation of the SiNW solution droplet, and the droplet encountered the masked and unmasked areas of the patterned substrate, respectively(shown in Fig. 4(a)). Due to the discrepancy in the surface energies of the SU-8-2002 and SiO_2/Si substrate, the contact angle of the SiNW droplet continuously changed when the SiNW ink

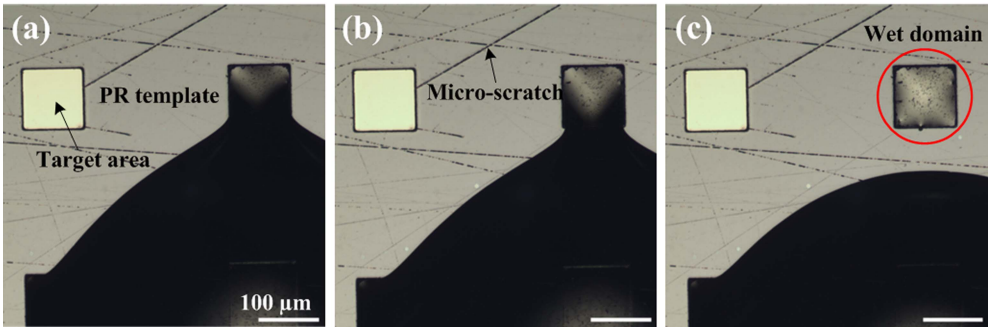

Fig. 3. (a)-(c) Optical microscope images showing the evaporating movement of DI water-based droplet containing SiNWs as a function of time. The small SiNW ink droplet is separated from the original ink droplet. All scale bars indicate 100 μm.

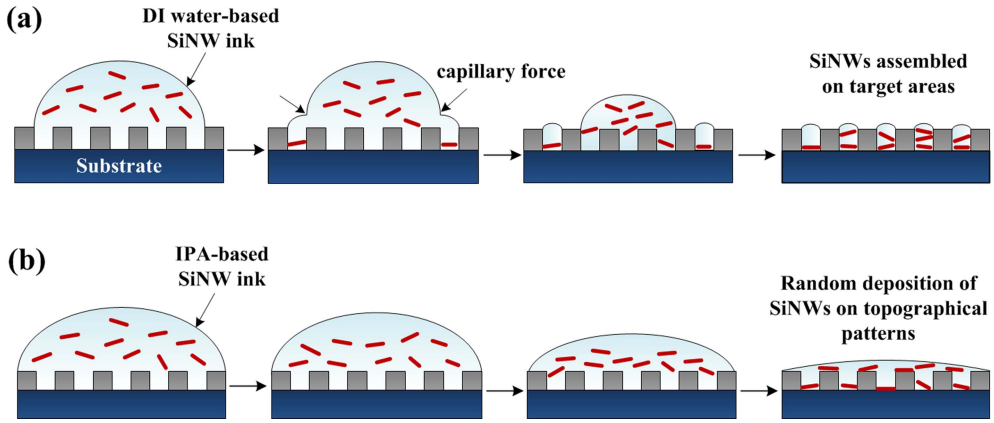

Fig. 4. Schematic representations of the moving behavior of SiNWs inside a droplet (a) at de-pinned contact mode and (b) at pinned contact mode.

encountered surfaces with different surface energies. In specific, when the edge of the SiNW solution droplet was located on the unmasked area of SiO_2 surface, the contact angle of the droplet decreased owing to the reduced surface energy. Whereas the contact line of the SiNW ink receded relatively fast when it was on the hydrophobic surface of SU-8-2002 patterns, the contact line was prone to be pinned on the hydrophilic surface of SiO_2 substrate. The droplet tried to resist the decrease in the contact area of the droplet, leading to the generation of capillary force and discontinuity of the droplet edge at the interface between the unmasked SiO_2 surface and SU-8 patterns, as denoted with arrows in Fig. 4(a). The contact line of the droplet receded due to the capillary force and a high local pressure, leaving the unmasked area filled with SiNW ink separated from the original SiNW solution droplet. This process was repeated during the entire evaporation process, and consequently the unmasked areas of SiO_2 surface were filled with SiNW ink; upon their evaporation, SiNWs were assembled as networks in the unmasked area.

In contrast, IPA evaporation on patterned substrate displayed a tendency of the pinned contact mode, which was occurred by the lower surface tension and faster evaporation rate than those of DI water. Unlike the evaporation of DI water-based SiNW solution, SiNW solution based on IPA evaporates while maintaining its original contact area and reducing its contact angle. The pinned contact mode of SiNW solution based on IPA resulted in random deposition of SiNWs regardless of the surface energy of the underlying layer. As shown in Fig. 4(b), the droplet contacted area of SiNW solution based on IPA is not affected by the pattern because the size of a droplet is larger than the size of the pattern, and droplet is fixed until the full evaporation. Therefore, SiNWs are deposited by the natural convection force inside SiNW ink, and in case of our experiment, SiNWs are evenly deposited.

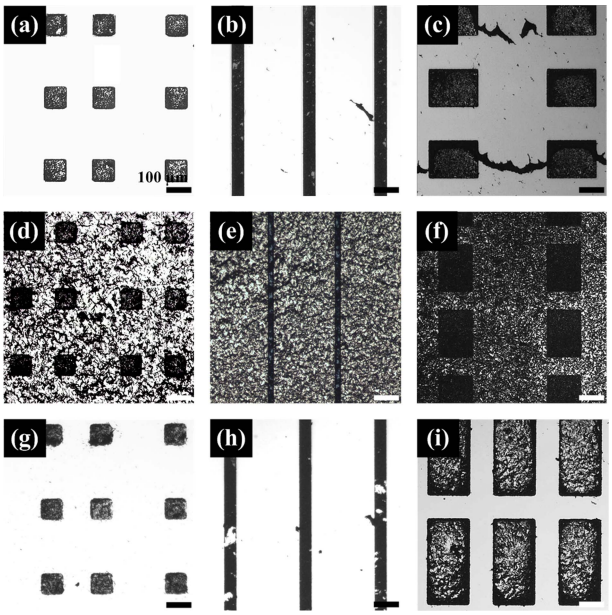

Fig. 5. Optical microscope images (a)-(f) before PR removing and (g)-(i) after PR removing. (d)-(f) represents optical microscope images of the middle part of the sample. All scale bars indicate 100 μm.

Fig. 5 shows the optical microscope images of the deposited SiNWs on diversely patterned substrates after the full evaporation of the solvent in DI water-based SiNW solution and SiNW solution based on IPA. As shown in Figs. 5(a)~(c), the SiNWs assembled by using the DI water-based SiNW solution were mostly placed in the unmasked area by the following the mechanism described in Fig. 4(a). The same SiNW agglomeration on PR surface observed in Figs. 5(b) and (c) was due to the micro-scratches on PR surface. Even though most SiNWs were well-collected in the unmasked area, SiNWs in the middle section of the patterned substrate were deposited on both the unmasked area and the masked area as

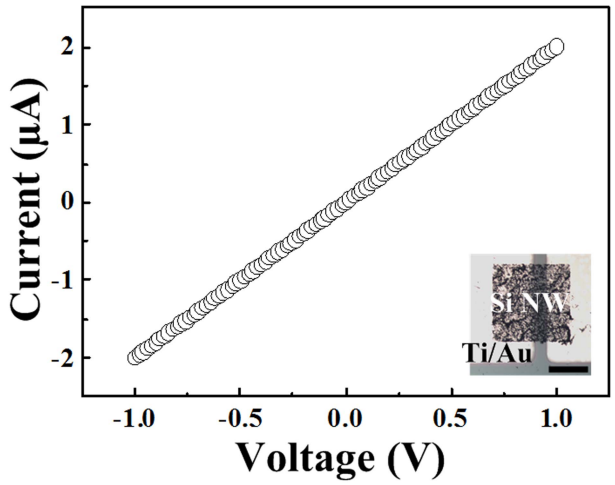

Fig. 6. Typical linear current versus voltage curves recorded from Si NW network. The resistance is 500 kΩ. Inset shows the optical microscope image of SiNW networks assembled on target area of SiO_2/Si substrate with two Ti/Au electrodes. Scale bar indicates 100 μm.

shown in Figs. 5(d)~(f). The different aspect of assembly depending on the position of the substrate can be attributed to frequent conversion of evaporation contact modes. The evaporation mode of a solution can be determined by the complex relationship between various factors including the evaporation rate, residual mass of the droplet, size of the droplet, surface tension, and etc.[22] In other words, a perfect evaporation mode is almost impossible and a instead mixed evaporation mode can be occurred instead. According to another research, the evaporation mode switching is due to the existence of contact angle hysteresis.[23] In the experiment with the DI water-based SiNW solution, the de-pinned contact mode was dominant at the most portion of the evaporation, but changes its mode to pinned contact mode at the last stage of the evaporation with a large concentration of SiNWs inside the droplet. Therefore, high density of SiNW suspension was dried in a state of covering all patterns which is placed in the middle part of the substrate with randomly deposited SiNWs over the substrate surface regardless of patterns. Since the portion of the middle part with equally deposited SiNWs is very small compared to the region of well-assembled SiNWs, it can be negligible or removed by a PDMS stamp. After SiNW networks had been obtained in the unmasked area, PR layers were removed in order to obtain SiNW networks on the bare substrate with desired structures and positions as shown in Figs. 5(g)~(i). The SU-8-2002 can be removed by a burning technique which is performed in a furnace at 450-500 ^{o}C for 2 min in an ambient atmosphere.

To confirm the compatibility with electronic devices, we have fabricated SiNW networks with Au/Ti electrodes (50 nn/10 nm) on 300 nm thick SiO_2/Si substrate, and measured the electrical transport. The *I-V* curve was obtained by sweeping the bias voltage with a 0.02V step, which exhibited linear current versus voltage relationship (Fig. 6). The calculated resistance was about 500 kΩ, which is a moderate resistance compared to the conventional SiNW network resistance ranging from 260 to 1780 kΩ.[15] As a result, we identified that this assembly method can produce electrically active SiNW network with diverse shapes on desirable location of the substrate.

4. Conclusion

In summary, we systematically investigated the assembly mechanism of SiNWs suspending in different solutions which make de-pinned and pinned contact modes on SU-8-2002 PR. We have showed that the behavior of SiNWs inside a droplet at de-pinned contact mode is affected by the convection force, evaporation direction, and different wettability between the relatively hydrophobic PR surfaces and relatively hydrophilic unmasked surfaces. After assembly of SiNWs, we performed a burning technique for removing PR layer without damaging and affecting assembled SiNWs in pre-defined regions. The measured *I-V* curve based on assembled SiNW networks showed an appropriate result showing linear current versus voltage relationship. The estimated resistance of SiNW networks is also in agreement with the resistance of conventional SiNW network. As a result, our technique can provide simple and effective way to accurately position SiNWs on desirable locations, which also can be applied to large-scale assembly of SiNWs with almost accuracy as long as assembly conditions are fulfilled, such as de-pinned contact mode on PR patterns and flawless PR surface without micro-scratches.

Acknowledgement

This work was supported by the Priority Research Centers Program through the National Research Foundation of Korea(NRF) funded by the Ministry of Education, Science and Technology(2012-0006689).

References

1. S. W. Chung, J. Y. Yu and J. R. Health, Appl. Phys. Lett., **76**, 2068 (2000).
2. Y. Cui and C. M. Lieber, Science, **291**(5505), 851 (2001).
3. G. Zheng, W. Lu, S. Jin and C. M. Lieber, Adv. Mater., **16**(21), 1890 (2004).
4. L. Tsakalakos, J. Balch, J. Fronheiser, B. Korevaar, O. Sulima and J. Rand, Appl. Phys. Lett., **91**, 233117 (2007).

5. Y. Lee, K. Kakushima, K. Shiraishi, K. Natori and H. Iwai, J. Appl. Phys., **107**, 113705 (2010).
6. P. A. Smith, C. D. Nordquist, T. N. Jackson, T. S. Mayer, B. R. Martin, J. Mbindyo and T. E. Mallouk, Appl. Phys. Lett., **77**(9), 1399 (2000).
7. M. Tanase, L. A. Bauer, A. Hultgren, D. M. Silevitch, L. Sun, D. H. Reich, P. C. Searson and G. J. Meyer, Nano Lett., **1**(3), 155 (2001).
8. B. Messer, J. H. Song and P. Yang, J. Am. Chem. Soc., **122**(41), 10232 (2000).
9. W. Salalha and E. Zussman, Phys. Fluids, **17**(6), 1 (2005).
10. J. Huang, R. Fan, S. Connor and P. Yang, Angew. Chem. Int. Edit., **46**(14), 2414 (2007).
11. A. J. Petsi, A. N. Kalarakis and V. N. Burganos, Chem. Eng. Sci., **65**(10), 2978 (2010).
12. P. Yang and F. Kim, ChemPhysChem, **3**(6), 503 (2002).
13. F. Kim, S. Kwan, J. Akana and P. Yang, J. Am. Chem. Soc., **123**(18), 4360 (2001).
14. A. R. Tao, J. Huang and P. Yang, Accounts Chem. Res., **41**(12), 1662 (2008).
15. D. Whang, S. Jin, Y. Wu and C. M. Lieber, Nano Lett., **3**(9), 1255 (2003).
16. Y. K. Kim, S. J. Park, J. P. Koo, D. J. Oh, G. T. Kim, S. Hong and J. S. Ha, Nanotechnology, **17**(5), 1375 (2006).
17. Z. Fan, J. C. Ho, Z. A. Jacobson, R. Yerushalmi, R. L. Alley, H. Razavi and A. Javey, Nano Lett., **8**(1), 20 (2008).
18. M. Lee, J. Im, B. Y. Lee, S. Myung, J. Kang, L. Huang, Y. K. Kwon and S. Hong, Nat. Nanotechnology, **1**(1), 66 (2006).
19. S. J. Oh, Y. Cheng, J. Zhang, H. Shimoda and O. Zhou, Appl. Phys. Lett., **82**(15), 2521 (2003).
20. K. Heo, E. Cho, J. E. Yang, M. H. Kim, M. Lee, B. Y. Lee, S. G. Kwon, M. S. Lee, M. H. Jo, H. J. Choi, T. Hyeon and S. Hong, Nano Lett., **8**(12), 4523 (2008).
21. S. Lee, J. H. Koo, J. Seo, S. D. Kim, K. H. Lee, S. Im, Y. W. Kim, T. Lee, J. Nanopart. Res., **14**, 840 (2012).
22. H. Y. Erbil, G. McHale, M. I. Newton, Langmuir, **18**(7), 2636 (2002).
23. R. Sharma, C. Y. Lee, J. H. Choi, K. Chen and M. S. Strano, Nano Lett., **7**(9), 2693 (2007).